Law of Localization in Chemical Reaction Networks

Takashi Okada and Atsushi Mochizuki

Phys. Rev. Lett. **117**, 048101 — Published 20 July 2016

DOI: 10.1103/PhysRevLett.117.048101

Law of Localization in Chemical Reaction Networks

Takashi Okada[1] and Atsushi Mochizuki[1,2]
[1] *Theoretical Biology Laboratory, RIKEN, Wako 351-0198, Japan*
[2] *CREST, JST 4-1-8 Honcho, Kawaguchi 332-0012, Japan*

In living cells, chemical reactions are connected by sharing their products and substrates, and form complex networks, e.g. metabolic pathways. Here we developed a theory to predict the sensitivity, i.e. the responses of concentrations and fluxes to perturbations of enzymes, from network structure alone. Responses turn out to exhibit two characteristic patterns, *localization* and *hierarchy*. We present a general theorem connecting sensitivity with network topology that explains these characteristic patterns. Our results imply that network topology is an origin of biological robustness. Finally, we suggest a strategy to determine real networks from experimental measurements.

PACS numbers: 02.10.Ud, 47.27.ed, 87.10.-e

Cells have many chemical reactions, each of which is mediated by organic catalysts, enzymes. Reactions are not independent but connected and form complex networks. Dynamics of chemical concentrations are considered as origin of physiological functions. However, dynamical behavior based on the network is not understood well.

One experimental approach to study such network systems is sensitivity analysis where amount/activity of enzymes are perturbed and responses (concentrations of chemicals in the system) are measured [1]. However, the result of such experiments are very difficult to interpret, because theoretical criteria to evaluate the results of perturbations from network structures are not established.

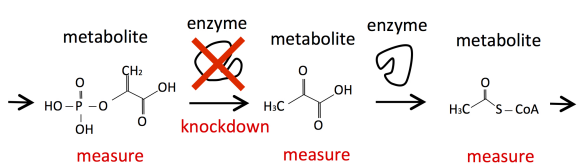

FIG. 1. Sensitivity analysis. After the amount/activity of an enzyme protein is decreased, the concentration change of metabolites are measured.

There are other difficulties to understand dynamical behaviors of reaction systems in biology. First, although huge information of reaction networks is available on databases [2–4], they provide no more than knowledge of identified reactions in biochemistry. It is possible that the information is incomplete, including many unidentified reactions or regulations. Second, in spite of the recent progress in biosciences, it is still difficult or almost impossible to determine quantitative details of dynamics, such as functions for reaction rates, parameter values, or initial states.

In order to circumvent these difficulties, we introduce a mathematical method, named *structural sensitivity analysis* [13, 14], to determine responses of chemical reaction systems to perturbation of enzyme amount/activity based only on network structure. From analyses we found that qualitative responses at a steady state is determined from information of network structure only. We also found that response patterns, e.g. distribution of nonzero responses of chemical concentrations in the network, exhibit two characteristic features, *localization* and *hierarchy* depending on the structure of networks and position of perturbed reactions. Finally we found a general theorem connecting the network topology and the response patterns directly, and governing the characteristic patterns of responses. This theorem, which we call the *law of localization*, is not only theoretically important, but also practically useful for examining real biological systems. In the context of adaptation, there were some previous studies, which reported confined nonzero responses in specific systems [9–12]. However, they did not find general laws of such response patterns, nor any topological conditions.

We study concentration changes in a reaction system under perturbation of reaction rate parameters, assuming that the system is in a steady state [13, 14]. We label chemicals by $m\,(m = 1, \cdots, M)$ and reactions by $j\,(j = 1, \cdots, R)$. A state of the system is specified by concentrations $x_m(t)$ and obeys the following differential equations [15, 16]

$$\frac{dx_m}{dt} = \sum_{i=1}^{R} \boldsymbol{\nu}_{mi} W_i(k_i; x). \tag{1}$$

Here, $\boldsymbol{\nu}$ is called a stoichiometric matrix. W_i is called a flux, which depends metabolite concentrations and also on a reaction rate k_i. We do not assume specific forms for W_i, but assume that each W_i is an increasing function of its substrate concentration;

$$\begin{cases} \frac{\partial W_i}{\partial x_m} > 0 & \text{if } x_m \text{ is a substrate of reaction } i, \\ \frac{\partial W_i}{\partial x_m} = 0 & \text{otherwise.} \end{cases} \tag{2}$$

Below, we abbreviate and emphasize *nonzero* $\frac{\partial W_i}{\partial x_m}$ as r_{im}.

In this framework, enzyme knockdown of the j-th reaction corresponds to changing the rate as $k_j \to k_j + \delta k_j$ (triangles in FIG. 2). By assuming steady state [5–8], the flux is expressed, in terms of a basis $\{\vec{c}_n\}$ of $\ker \boldsymbol{\nu}$,

as $\vec{W} = \sum_{n=1}^{N_k} \mu^n \vec{c}_n$, where N_k is the dimension of the kernel and μ^n are N_k coefficients depending on reaction rates. Under the j-th knockdown, we have

$$\delta_j \vec{W} = \sum_{n=1}^{N_k} \delta_j \mu^n \vec{c}_n = \left(\sum_{n=1}^{N_k} \frac{d\mu^n}{dk_j} \vec{c}_n \right) \delta k_j. \tag{3}$$

The i-th component of $\delta_j \vec{W}$ is also expanded as

$$\delta_j W_i = \left(\frac{\partial W_i}{\partial k_j} + \sum_{m'=1}^{M} \frac{\partial W_i}{\partial x_{m'}} \frac{dx_{m'}}{dk_j} \right) \delta k_j. \tag{4}$$

From (3) (4), the response of steady state concentration $\delta_j \vec{x} \equiv \frac{d\vec{x}}{dk_j} \delta k_j$ (circles in FIG. 2) and flux $\delta_j \vec{W}$ (arrows in FIG. 2) to each perturbation $k_j \to k_j + \delta k_j$ is determined from network structure only [13, 14]. The result for each perturbation is simultaneously obtained through the following matrix computation:

$$\left(\begin{array}{c|c} \delta_1 \vec{x} \;\; \delta_2 \vec{x} \;\; \cdots \delta_R \vec{x} \\ \hline \delta_1 \vec{\mu} \;\; \delta_2 \vec{\mu} \;\; \cdots \delta_R \vec{\mu} \end{array} \right) \propto \mathbf{A}^{-1} \equiv \mathbf{S} \tag{5}$$

where the matrix $\mathbf{A}$ is given as

$$\mathbf{A} = \left(\begin{array}{c|ccc} \frac{\partial W_i}{\partial x_m} & -\vec{c}_1 & \cdots & -\vec{c}_{N_k} \end{array} \right). \tag{6}$$

In (5) and (6), the horizontal and vertical lines are the partitions of the matrices. We then obtain the flux change $\delta_j \vec{W}$ from (3), or

$$\left(\delta_1 \vec{W} \cdots \delta_R \vec{W} \right) = \left(\vec{c}_1 \cdots \vec{c}_{N_k} \right) \left(\delta_1 \vec{\mu} \cdots \delta_R \vec{\mu} \right) \tag{7}$$

in a matrix notation. We call the inverse of $\mathbf{A}$ as the *sensitivity matrix* $\mathbf{S}$. Note that $\delta_j \vec{x}$, $\delta_j \vec{\mu}$, $\delta_j \vec{W}$, $\vec{c}_n$ are column vectors with M, N_k, R, and R components respectively, and $\frac{\partial W_i}{\partial x_m}$ is an R-by-M matrix. We assume networks with $\dim \ker \boldsymbol{\nu}^T = 0$ throughout this paper, which guarantees the matrix $\mathbf{A}$ is square, i.e. $R = M + N_k$.

Comments are in order. First, our theory depends only on the structure of reaction networks. The network structure is reflected in the distribution of nonzero entries in the $\mathbf{A}$-matrix, which determines the qualitative responses. Second, as a generalization of our method, we account for regulations such as allosteric effects by relaxing (2) as

$$\begin{cases} \frac{\partial W_i}{\partial x_m} \neq 0 & \text{if } x_m \text{ influences reaction } i, \\ \frac{\partial W_i}{\partial x_m} = 0 & \text{otherwise.} \end{cases} \tag{2'}$$

Then, regulations add additional r_{im} in the $\mathbf{A}$-matrix, and the response is still determined through (5).

Let us see some results of structural sensitivity analysis.

Example 1: We consider a straight pathway, shown in FIG. 2 (Left). The $\mathbf{A}$-matrix and the sensitivity matrix $\mathbf{S}$ are

$$\mathbf{A} = \left(\begin{array}{cc|c} 0 & 0 & -1 \\ r_{2A} & 0 & -1 \\ 0 & r_{3B} & -1 \end{array} \right), \mathbf{S} = \left(\begin{array}{ccc} -r_{2A}^{-1} & r_{2A}^{-1} & 0 \\ -r_{3B}^{-1} & 0 & r_{3B}^{-1} \\ \hline -1 & 0 & 0 \end{array} \right). \tag{8}$$

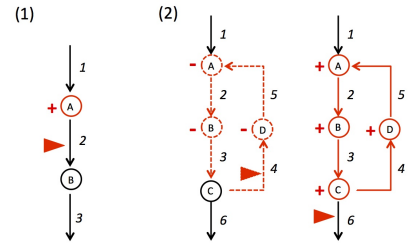

FIG. 2. Reaction networks and sensitivities in Example 1 and 2. The red triangle indicates a knocked down reaction. The signs (increase/decrease) of responses are represented by $+/-$ for chemicals and solid/dashed red lines for fluxes.

The flux changes only when we perturb the top reaction 1 (the 1st column of $\mathbf{S}$). The perturbation to reactions 2 or 3 changes only its substrate concentration (the 2nd, 3rd column of $\mathbf{S}$).

Example 2: The second example shown in FIG. 2 (Right) consists of 6 reactions and 4 chemicals.The matrices $\mathbf{A}$ and $\mathbf{S}$ are

$$\mathbf{A} = \left(\begin{array}{cccc|cc} 0 & 0 & 0 & 0 & -1 & 0 \\ r_{2A} & 0 & 0 & 0 & -1 & -1 \\ 0 & r_{3B} & 0 & 0 & -1 & -1 \\ 0 & 0 & r_{4C} & 0 & 0 & -1 \\ 0 & 0 & 0 & r_{5D} & 0 & -1 \\ 0 & 0 & r_{6C} & 0 & -1 & 0 \end{array} \right), \tag{9}$$

$$\mathbf{S} = \left(\begin{array}{cccccc} \frac{-r_{4C}-r_{6C}}{r_{2A}r_{6C}} & r_{2A}^{-1} & 0 & -r_{2A}^{-1} & 0 & \frac{r_{4C}}{r_{2A}r_{6C}} \\ \frac{-r_{4C}-r_{6C}}{r_{3B}r_{6C}} & 0 & r_{3B}^{-1} & -r_{3B}^{-1} & 0 & \frac{r_{4C}}{r_{3B}r_{6C}} \\ -\frac{1}{r_{6C}} & 0 & 0 & 0 & 0 & r_{6C}^{-1} \\ -\frac{r_{4C}}{r_{5D}r_{6C}} & 0 & 0 & -r_{5D}^{-1} & r_{5D}^{-1} & \frac{r_{4C}}{r_{5D}r_{6C}} \\ \hline -1 & 0 & 0 & 0 & 0 & 0 \\ -\frac{r_{4C}}{r_{6C}} & 0 & 0 & -1 & 0 & \frac{r_{4C}}{r_{6C}}. \end{array} \right). \tag{10}$$

Again, only the perturbation to the input rate, corresponding to the 1st column in (10), affect all chemicals and fluxes. Perturbations to reactions $2, 3, 5$ only decrease the concentrations of the substrates A, B, D respectively. Knockdown of reaction 4 decreases the concentrations D, A, B along the cycle downward of the perturbation (see FIG. 2, and the 4th column of $\mathbf{S}$). Knockdown of reaction 6 doe not change the further downstream but change A, B, C, D in the cycle. Also, the signs of the responses are reversed (the 6th column of $\mathbf{S}$).

Example 3: The third network in FIG. 3 (Left) includes 10 chemicals and 15 reactions. FIG. 3 (Right) shows nonzero response patterns of metabolites and inclusion relation between them. See Supplementary Material (SM) for the $\mathbf{A}$-matrix and the sensitivity matrix.

In general, response to perturbations in chemical reaction networks exhibits two characteristics, *localization* and *hierarchy*. The *localization* means that the influence of the perturbations is confined in a finite region in a network. In other words, the naive intuition that a perturbation in an upper part of a reaction network influences all of the lower parts is incorrect. The *hierarchy* implies that the nonzero response patterns under perturbations of different reaction rates exhibit inclusion relations among them.

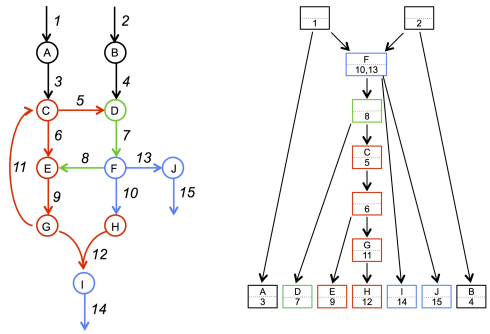

FIG. 3. (Left) Reaction network of example 3. (Right) Graph of response hierarchy, summarizing the inclusion relations between nonzero response patterns. When a reaction rate in any square box is perturbed, the metabolites in the box plus those in the lower boxes shows nonzero responses. The three colors (red, green, blue) correspond to $\Gamma_{10}, \Gamma_{11}, \Gamma_{12}$ respectively in the text.

From the $\mathbf{A}$-matrix (6), we can generally prove a theorem, the *law of localization*, that determines the extent to which a perturbation influences in a network. For a given network, we consider a pair $\Gamma = (\mathfrak{m}, \mathfrak{r})$ of a metabolite subset $\mathfrak{m}$ and a reaction subset $\mathfrak{r}$ satisfying the condition that $\mathfrak{r}$ includes all reactions influenced by metabolites in $\mathfrak{m}$ (see the condition (2')). The choice of $\mathfrak{r}$ for a chosen $\mathfrak{m}$ is not unique in general. We call a subnetwork satisfying this condition "output-complete". For such a subnetwork Γ, we count the number $|\mathfrak{m}|$ of elements in $\mathfrak{m}$, the number $|\mathfrak{r}|$ of elements in $\mathfrak{r}$, and the number $N_k(\mathfrak{r})$ of the closed cycles that consist of the reaction subset $\mathfrak{r}$. Then, we compute a index,

$$\lambda(\Gamma) \equiv -|\mathfrak{m}| + |\mathfrak{r}| - N_k(\mathfrak{r}), \tag{11}$$

which is analogous to Euler characteristic and generally non-negative. The *law of localization* states that if $\lambda(\Gamma) = 0$ for an output-complete subnetwork Γ, then any perturbation of reactions in Γ does not change the concentrations and the fluxes outside of Γ, namely the perturbation effect is localized in Γ itself. We call an output-complete subnetwork satisfying $\lambda(\Gamma) = 0$ as a *buffering structure*.

(Proof): The theorem is proved from the distribution of nonzero entries of the $\mathbf{A}$-matrix. (i) Suppose a subnetwork Γ is a buffering structure. Then by appropriately choosing a basis of the kernel of $\boldsymbol{\nu}$ and the orderings of the indices of the $\mathbf{A}$-matrix, we can always rewrite the $\mathbf{A}$-matrix as,

$$\mathbf{A} = \begin{array}{c} \\ |\mathfrak{r}| \end{array} \overset{|\mathfrak{m}|+N_k(\mathfrak{r})}{\left(\begin{array}{c|c} \underset{square}{*} & * \\ \hline \mathbf{0} & * \end{array}\right)}. \tag{12}$$

The lower left block vanishes because $\mathbf{A}$ is output-complete. (ii) As explained already, the concentration change $\delta_j x_m$ is proportional to $\mathbf{A}^{-1}_{mj} \propto \mathrm{Det}\, \hat{\mathbf{A}}^{(j;m)}$, where $\hat{\mathbf{A}}^{(j;m)}$ is the minor matrix associated with the row of the j-th reaction and the column of the m-th metabolite. Then, $\mathrm{Det}\, \hat{A}^{(j;m)} = 0$ for $i \in \mathfrak{r}$, $m \notin \mathfrak{m}$ follows because the upper left block in the minor $\hat{\mathbf{A}}^{(j;m)}$, which was originally square in (12), is horizontally long. □

We illustrate the *law of localization* in the example networks in FIG. 2 and FIG. 3 (Left).

Example 1: The network includes two buffering structures, $\Gamma_1 = (\{A\}, \{2\})$ and $\Gamma_2 = (\{B\}, \{3\})$ which are minimum buffering structures including only a single chemical and a single output reaction. The *law of localization* claims that the perturbation to reaction 2 in Γ_1 should influence only inside of Γ_1, namely the concentration of A (since the flux 2 should not change in order to keep the outside of Γ_1 unchanged). We actually observed the predicted response in (8). Generally, a perturbation to a reaction which is a single output from a chemical influences the substrate concentration only.

Example 2: In addition to the 3 minimal buffering structures, $\Gamma_1 = (\{A\}, \{2\})$, $\Gamma_2 = (\{B\}, \{3\})$, $\Gamma_3 = (\{D\}, \{5\})$, the network has two larger ones, $\Gamma_4 = (\{A, B, D\}, \{2, 3, 4, 5\})$ (with $\lambda(\Gamma_4) = -3 + 4 - 1 = 0$), $\Gamma_5 = (\{A, B, C, D\}, \{2, 3, 4, 5, 6\})$ (with $\lambda(\Gamma_5) = -4+5-1 = 0$). Γ_4 is the minimum buffering structure including reaction 4. Then, the *law of localization* predicts that the nonzero response to perturbation of reaction 4 should be limited within Γ_4, which is observed in the 4th column in (10). Similarly, the response to perturbation of reaction 6 is explained by Γ_5.

Example 3: The network has 14 buffering structures, listed in SM. To examine the response hierarchy, we focus on the three buffering structures colored in FIG. 3; $\Gamma_{10} = (\{C, E, G, H\}, \{5, 6, 9, 11, 12\})$ (with $\lambda(\Gamma_{10}) = -4 + 5 - 1 = 0$), $\Gamma_{11} = (\{C, D, E, G, H\}, \{5, 6, 7, 8, 9, 11, 12\})$ (with $\lambda(\Gamma_{11}) = -5 + 7 - 2 = 0$), and $\Gamma_{12} = (\{C, D, E, F, G, H, I, J\}, \{5, 6, 7, 8, 9, 10, 11, 12, 13, 14, 15\})$ (with $\lambda(\Gamma_{12}) = -8 + 11 - 3 = 0$). Each of these three explains the response pattern under perturbation of reaction 5, 8, and 10 (or 13), respectively, and they satisfy an inclusion relation, $\Gamma_{10} \subset \Gamma_{11} \subset \Gamma_{12}$. Accordingly, we can see from FIG. 3 (Right) that these response patterns satisfy an inclusion relation.

In this way, we understand all of the observed patterns from network topology by using the *law of localization*. In short, the first characteristic, *localization*, is explained from existence of buffering structures. The second property, *hierarchy*, is explained as the nest of the buffering structures.

Finally, as an application to real biological networks, we examine the carbon metabolism pathway of E. coli. The network is a major part of energy acquisition process, and the basic structures are shared between bacteria and human beings. FIG. 4 shows the network [1], including 28 metabolites and 46 reactions, and FIG . 5 shows

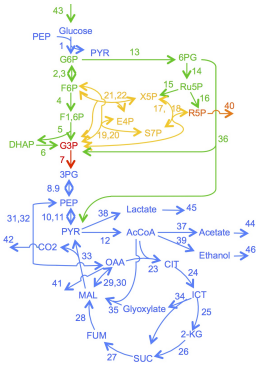

FIG. 4. E. coli network. (Adopted from [1]).

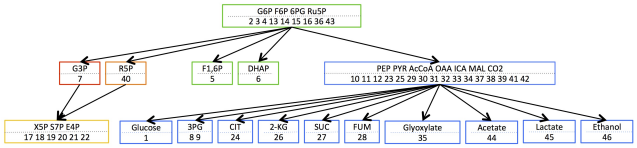

FIG. 5. The response hierarchy of E. coli network.

the response hierarchy (see SM for the detail). Again, the response patterns exhibit the two characteristic features, *localization* and *hierarchy*. The network has 17 buffering structures, and the existence and the nest of them explain the two characteristic features perfectly. We mention that some of the buffering structures, which are of course defined from network topology, are surprisingly overlapping to biologically identified sub-circuits, the pentose phosphate pathway (yellow in FIG. 4, 5), the tricarboxylic acid cycle (blue) and the glycolysis (green). This correspondence may be understood from an evolutional point of view by considering the advantage of buffering structures.

We discuss the biological significances of buffering structures (and nest of them) in two different levels. The first discussion is on the physiological importance. A buffering structure prohibits influence of given perturbation from expanding to the outside, like a "firewall". In other words, it is a substructure with robustness emerging from the network topology. The carbon metabolism network of E. coli possesses multiple nested firewalls (FIG. 5), and are expected robust to fluctuations of enzymes in it. We expect that such topological characteristic of reaction networks could be evolutionary origin of homeostasis of biological systems. A set of chemical reactions satisfying the condition of buffering structure by chance in evolutionarily early time would be positively selected as an advantageous circuit. We then expect that buffering structures in existing biological networks today might be generated and selected in such ways.

The second discussion is about practicality of the *law of localization* in experimental biology. Our knowledge of biochemical networks is considered incomplete: There might exist unidentified reactions or regulations. The condition for buffering structure depends on the local network structure only, which implies that we can study the sensitivity of the system only from local information on the network.

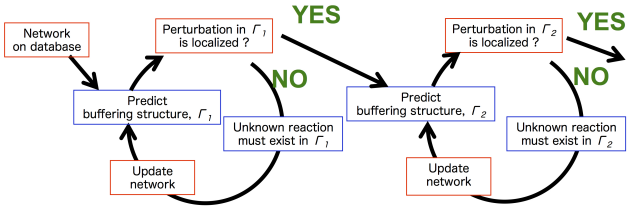

FIG. 6. A strategy toward elucidating a true network.

From this property, we can determine a "true" network by combining experiments as shown in FIG. 6. If a given perturbation (knock down or over expression) to a predicted buffering structure, determined from network topology, DOES influence outside of the buffering structure, then there must be inconsistency between the database information and the actual network. The mismatch must exist inside of the candidate structure, i.e. there must be unknown reactions or unknown regulations inside (or emanating from) the candidate subnetwork. By repeating theoretical predictions and experimental verifications, we can determine the "true" network from partial to the whole network in a step-by-step manner, i.e. from smaller to larger buffering structures. Our theory must promote understanding of reaction networks in both theoretical and experimental levels by directly connecting network topology with behaviors of the systems.

Using a different method, Steuer et al. studied a mathematical criteria for "perfect adaptation", where changing a rate constant in one part of the network does not affect steady-state concentrations or fluxes, which in fact, is a subpart of the phenomena we studied in this paper. There are at least three large differences: (i) We studied not only perfect adaptation, but also any qualitative responses (increase/decrease/invariant), (ii) While Steuer et al.'s method needs to examine a condition one by one for each pair of perturbation and chemicals, our method determines changes of all concentrations and fluxes by each perturbation of all reaction rates simultaneously via (5). (iii) We found and proved a general law which claims that the property of perfect adaptation emerges from local topology of network. Despite these differences, it would be interesting to explore relations between two mathematical theories.

This work was supported partly by the CREST, Japan Science and Technology Agency, and by iTHES research program RIKEN, by Grant-in-Aid for Scientific Research on Innovative Area, "Logics of Plant Development", Grant number 25113005. We greatly appreciate Bernold Fiedler, Hiroshi Matano, and Hannes Stuke for their mathematical discussions. We also express our sincere thanks to Testuo Hatsuda, Michio Hiroshima, Yoh Iwasa, Sinya Kuroda, Masaki Matsumoto, Keiichi Nakayama, Madan Rao, and Yasushi Sako for their helpful discussions and comments.

[1] Ishii, N., Nakahigashi, K., Baba, T., Robert, M., Soga, T., Kanai, A., Tomita, M. (2007). Multiple high-throughput analyses monitor the response of E. coli to perturbations. Science, 316(5824), 593-597.

[2] Ogata, H., Goto, S., Sato, K., Fujibuchi, W., Bono, H., Kanehisa, M. (1999). KEGG: Kyoto encyclopedia of genes and genomes. Nucleic acids research, 27(1), 29-34.

[3] Joshi-Tope, G., Gillespie, M., Vastrik, I., D'Eustachio, P., Schmidt, E., de Bono, B., Stein, L. (2005). Reactome: a knowledgebase of biological pathways. Nucleic acids research, 33(suppl 1), D428-D432.

[4] Karp, P. D., Ouzounis, C. A., Moore-Kochlacs, C., Goldovsky, L., Kaipa, P., Ahrén, D., López-Bigas, N. (2005). Expansion of the BioCyc collection of pathway/genome databases to 160 genomes. Nucleic acids research, 33(19), 6083-6089.

[5] Varma, A., Boesch, B. W., Palsson, B. O. (1993). Stoichiometric interpretation of Escherichia coli glucose catabolism under various oxygenation rates. Applied and environmental microbiology, 59(8), 2465-2473.

[6] Edwards, J. S., Palsson, B. O. (2000). The Escherichia coli MG1655 in silico metabolic genotype: its definition, characteristics, and capabilities. Proceedings of the National Academy of Sciences, 97(10), 5528-5533.

[7] Kauffman, K. J., Prakash, P., Edwards, J. S. (2003). Advances in flux balance analysis. Current opinion in biotechnology, 14(5), 491-496.

[8] Orth, J. D., Thiele, I., Palsson, B. O. (2010). What is flux balance analysis?. Nature biotechnology, 28(3), 245-248.

[9] Ni, Xiao Yu, Tormod Drengstig, and Peter Ruoff. The control of the controller: molecular mechanisms for robust perfect adaptation and temperature compensation. Biophysical journal 97.5 (2009): 1244-1253.

[10] Steuer, Ralf, et al. Robust signal processing in living cells. PLoS Comput Biol 7.11 (2011): e1002218.

[11] Drengstig, T., et al. A basic set of homeostatic controller motifs. Biophysical journal 103.9 (2012): 2000-2010.

[12] He, Fei, Vincent Fromion, and Hans V. Westerhoff. Perfect robustness and adaptation of metabolic networks subject to metabolic and gene-expression regulation: marrying control engineering with metabolic control analysis. BMC systems biology 7.1 (2013): 131.

[13] Mochizuki, A., Fiedler, B. (2015). Sensitivity of chemical reaction networks: A structural approach. 1. Examples and the carbon metabolic network. Journal of theoretical biology, 367, 189-202.

[14] Fiedler B., Mochizuki A. (2015). Sensitivity of Chemical Reaction Networks: A Structural Approach. 2. Regular Monomolecular Systems. Math. Meth. Appl. Sci. 38, 3381-3600.

[15] Craciun G., Feinberg M. (2006) Multiple equilibria in complex chemical reaction networks: The species-reactions graph. SIAM J. App. Math. 66:4, 1321-1338.

[16] Feinberg M. (1995) The existence and uniqueness of steady states for a class of chemical reaction networks. Arch. Rational Mech. Anal. 132, 311-370.